Volume 126, number 6 CHEMICAL PHYSICS LETTERS 23 May 1986

VIBRATIONAL PREDISSOCIATION INDUCED BY EXCITON TRAPPING IN INERT-GAS CLUSTERS

Dafna SCHARF, Joshua JORTNER
School of Chemistry, Tel-Aviv University, 69978 Tel Aviv, Israel

and

Uzi LANDMAN
School of Physics, Georgia Institute of Technology, Atlanta, GA 30322, USA

Received 10 February 1986

The dynamics of exciton trapping, vibrational energy transfer and vibrational predissociation in an electronically excited state of Ar_{13} clusters was explored by classical molecular dynamics. Two distinct time scales were established for vibrational energy flow, which result in a molecular-type, reactive dissociation process of Ar atoms for this cluster.

The processes of energy acquisition, storage and disposal in clusters are of considerable interest for the elucidation of dynamic processes in finite systems, whose energy spectrum for electronic and nuclear excitations can be varied continuously by changing the cluster size [1]. In this context, an important issue involves the consequences of vibrational excitations of clusters. Such relaxation processes fall into two categories: (i) non-reactive vibrational energy redistribution in the cluster, which does not result in dissociation, and (ii) reactive dissociation or vibrational predissociation. The mechanisms of vibrational energy acquisition by a cluster can involve collisional excitation, optical photoselective vibrational excitation or electronic excitation followed by the degradation of electronic energy into vibrational energy. In charged clusters, the vibrational excitation resulting in both non-reactive and reactive relaxation, can originate from ionization followed by hole trapping in inert-gas clusters [2–5] and from electron attachment to alkali halide clusters [6]. Information regarding the reactive consequences of vibrational excitation of small neutral clusters in their ground electronic state stems from two sources. First, molecular dynamics computer simulations of the dissociation of Ar_n ($n = 4$–6) clusters [7] can be accounted for in terms of the statistical theory of unimolecular reactions [8], which implies the occurrence of vibrational energy randomization in small clusters. Second, experimental molecular beam studies of optically vibrationally excited hydrogen-bonded $(HF)_n$ ($n = 2$–6) clusters [9] yield a lower limit of $> 10^6\ s^{-1}$ for the vibrational predissociation rate at the excess vibrational energy of 3000 cm^{-1}, and do not yet provide information on the interesting issue of intramolecular vibrational energy redistribution in these systems. The non-reactive and reactive processes induced by the degradation of electronic energy into vibrational energy in clusters have not yet been elucidated. An interesting problem in this category involves the dynamical consequences of exciton trapping in rare-gas clusters (RGCs), which is the subject matter of this note. Extensive information is currently available regarding exciton trapping in solid and liquid inert gases [10]. Exciton trapping in the heavy rare-gas solids, i.e. Ar, Kr and Xe, exhibits two-centre localization, resulting in the formation of electronically excited, diatomic rare-gas excimer molecules. Electronic excitation of a RGC, R_n, is expected to result in an exciton state, which subsequently becomes trapped by self-localization. Although the details of the energetics and spatial charge distribution of excitons in finite RGCs have not yet been explored, some information can be drawn from the analogy with the lowest electronic excitations in solid and liquid rare gases, which can adequately be described [10] either in terms of intermediate Wannier exciton states with large central cell corrections, or by strongly perturbed Frenkel excitons. Adopting the latter approach, the two lowest, dipole allowed, electronic excitations in RGCs can adequately be described in terms of tightly bound, Frenkel-type excitations with a parentage in the ${}^1S_1 \rightarrow {}^3P_1$ and ${}^1S_0 \rightarrow {}^1P_1$ atomic excitations, which are modified by large non-orthogonality corrections [10]. The energetic separation between these two electronic excitations corresponds to the spin–orbit splitting [10]. This description of the electronic excitations rests on a decidedly molecular description. An analogous molecular point of view [11] is adopted for the description of exciton trapping in RGCs. The process of exciton trapping in the heavy RGCs of Ar, Kr and Xe involves the formation of the diatomic excimer molecule R_2^*, which is characterized by a substantial binding energy for a high vibrational state. Energy exchange between the R_2^* excimer and the cluster in which it is embedded involves two processes:

(1) Short-range repulsive interactions between the expanded, Rydberg-type excited state of the excimer and the other cluster atoms result in a dilation of the local structure around the excimer, leading to energy flow into the cluster.

(2) Vibrational relaxation of the excimer induces vibrational energy flow into the cluster.

The vibrational energy released into the cluster by processes (1) and (2) may result in vibrational predissociation.

We have explored the dynamic implications of exciton trapping in RGCs by conducting classical molecular dynamics (MD) calculations [12,13] on electronically excited states of such clusters. Applications of MD to photophysical processes start to emerge. MD simulations of photochemical dissociation and radical back recombination in clusters were recently reported [14]. The present work constitutes an application of the MD technique for the dynamics of electronically–vibrationally excited states of large systems. As a model system we have chosen the Ar_{13} cluster. Our calculations are based on additive pairwise interactions. The ground states of the RGCs have been described by additive Lennard-Jones pair potentials, $V(r) = 4\epsilon[(\sigma/r)^{12} - (\sigma/r)^6]$, which are specified by $\epsilon = 121$ K and $\sigma = 3.40$ Å [15]. In the electronically excited state the Ar_2^* excimer potential is represented by a Morse curve, $V(r) = D_e\{\exp[-2B(r/R_e - 1)] - 2\exp[-B(r/R_e - 1)]\}$ with the parameters $D_e = 0.78$ eV, $R_e = 2.32$ Å and $B = 5.12$ [16]. An important consequence of the electronic excitation involves the drastic modification of the interaction between the excimer and the ground-state atoms. On the basis of the analysis of Xe*–Ar interactions [17], the Ar*–Ar potential for each of the constituents of the excimer has been described in terms of a Lennard-Jones potential with the parameters ϵ^* and σ^*. We have taken for the energy $\epsilon^* = \epsilon$, while the distance scale ratio $\bar{\sigma} = \bar{\sigma}^*/\sigma$ has been chosen in the range $\bar{\sigma} = 1.0$–1.2. The appropriate Ar*–Ar interaction is characterized by [17] $\bar{\sigma} = 1.10$–1.15, reflecting the enhancement of short-range repulsive interactions in the electronically excited Rydberg-type state.

The ground-state equilibrium configuration of Ar_{13} was generated following a lengthy equilibration (5×10^4 integration steps) at a temperature $T = 24$ K, which is lower than the melting temperature ($T \approx 40$ K) [18–20] of this cluster. We find that at this temperature the Ar_{13} cluster assumes the icosahedron structure, which is in accord with previous results [20, 21]. Electronic excitation was performed on a particular equilibrated ground-state cluster configuration. The electronic excitation was achieved (at the time $t = 0$) by the instantaneous switching on of the excimer potential between a pair of atoms and of the Ar*–Ar potentials between the excimer and the ground-state atoms. We have adopted a local picture, disregarding the effects of electronic energy transfer within the cluster.

A fifth-order predictor–corrector method, which constitutes a very accurate version of the MD algorithm [22] has been used. The time increment in the ground state was $\Delta t = 1.6 \times 10^{-14}$ s. The larger forces and the abrupt velocity changes in the system following electronic excitation require shorter time increments. Accordingly, we have used $\Delta t = 1.6 \times 10^{-16}$–$5.0 \times 10^{-16}$ s in this electronically excited state. In all our MD calculations conservation of energy prevailed with an accuracy of 1 ppm.

In figs. 1a and 1b we show an overview of the dynamics of the nuclear motion following the electron-

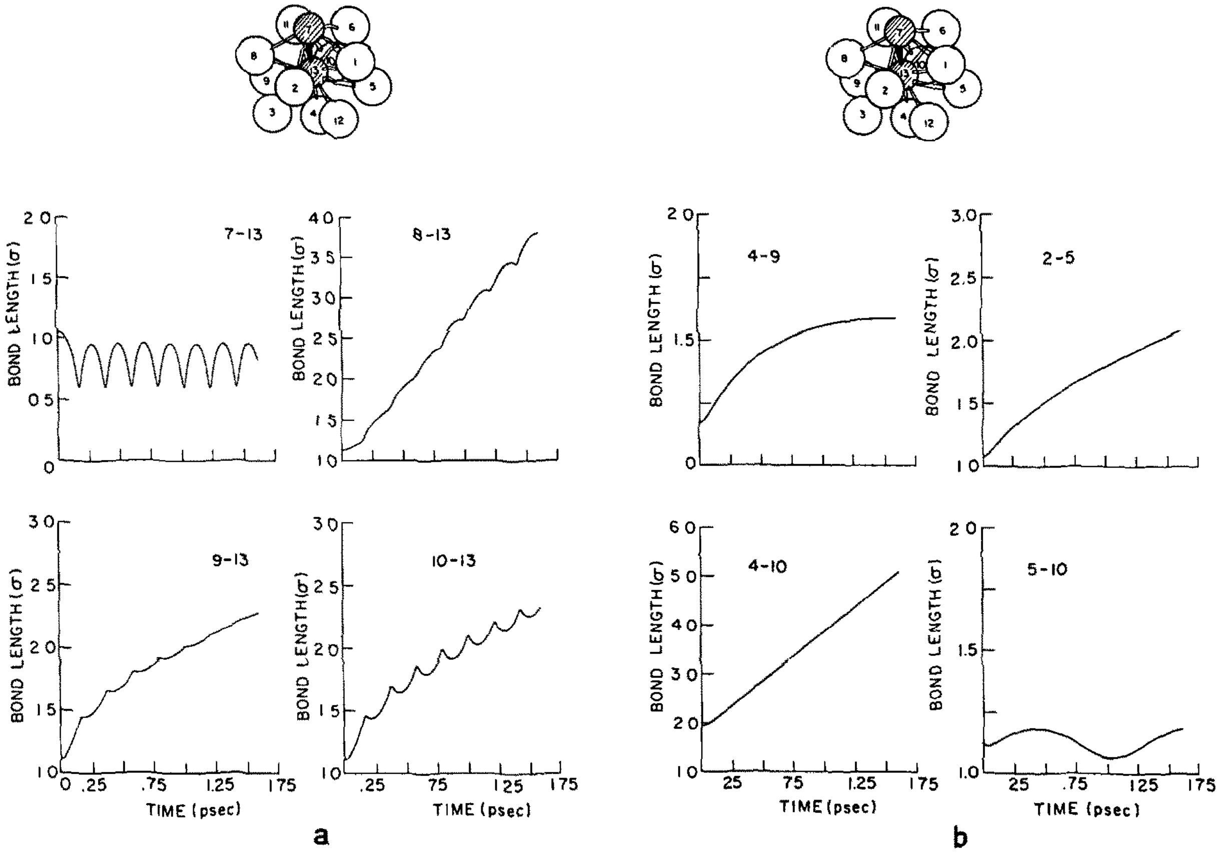

Fig. 1. Time dependence of interatomic distances in the electronically excited Ar$^*_{13}$ cluster. The insert shows the ground-state equilibrium structure at 24 K. The labelling of atoms is indicated. The dashed atoms 7 and 13 form the excimer. Distances are in units of σ. The Ar*–Ar interaction is characterized by $\bar{\sigma} = 1.20$. (a) Interatomic distances within the excimer and between the excimer atoms and some ground-state atoms. (b) Interatomic potentials between some ground-state atoms.

ic excitations, which is expressed in terms of the interatomic distances. The excimer exhibits a large-amplitude motion in a highly excited vibrational state, while all the other interatomic distances increase, indicating the initiation of the escape of the ground-state cluster atoms. Insight into the energy flow from the excimer into the cluster is obtained from the time dependence of the kinetic energy (KE), the potential energy (PE) and the total energy of the excimer (fig. 2). The strong oscillations in the PE and KE clearly indicate the persistence of the vibrational excitation of the excimer over a long time scale. Further detailed information concerning the implications of this energy flow on the cluster dissociation was inferred by considering the composition and the energetics of the "main fragment", i.e. the fragment which consists of the excimer together with ground-state atoms, with all the nearest-neighbour separations being smaller than 3σ, beyond which all interatomic interactions are negligibly small. The total energy within the main fragment was partitioned into two separate contributions: (i) the energy of the "reaction centre", which consists of the excimer PE and KE together with half of the sum of the potential energy of the Ar*–Ar interactions, and (ii) the energy of the "bath subsystem", which involves the KE of the ground-state Ar atoms,

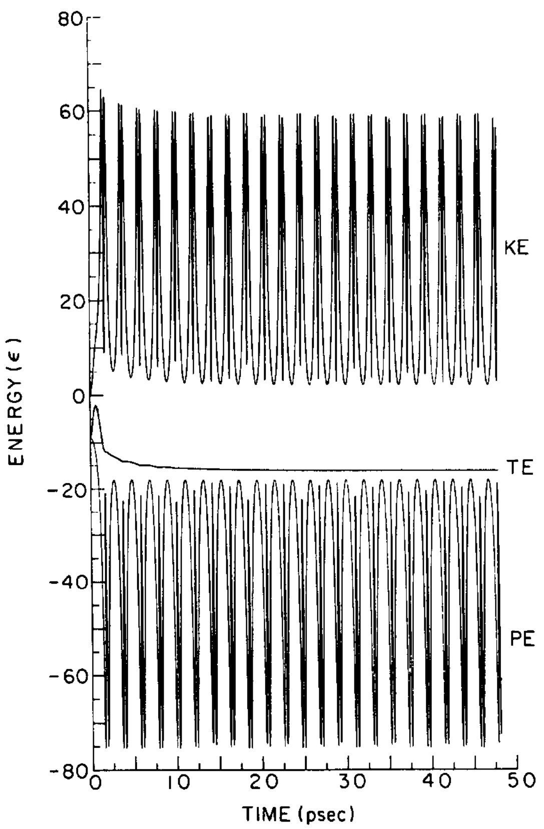

Fig. 2. Time dependence of the potential energy (PE), the kinetic energy (KE) and the total energy (TE) of the bare excimer in Ar_{13} ($\bar{\sigma} = 1.20$). Energies are given in units of ϵ.

the potential energies of the Ar–Ar interactions and half of the sum of the potential energies of the Ar^*–Ar interactions. The time evolution of the various contributions to the total energy (fig. 3) portray the energy flow from the excitation centre into the "bath". However, the energy per atom does not equilibrate. Discontinuities (i.e. "steps") in the energy plots of fig. 3 mark the dissociation of the main fragment, with the decrease of the total energy corresponding to the KE of the ground-state atoms dissociating from it. A cursory examination of the time evolution of the composition of the main fragment (fig. 3) clearly indicates that the major fragmentation process involves the sequential stepwise dissociation, i.e. "evaporation", of single ground-state atoms from the main fragment. The escape of the excimer from the main fragment has not been encountered. The dissociation process is dominated by the magnitude of the excited-state potential scale parameter $\bar{\sigma}$. For realistic values [17] of $\bar{\sigma} = 1.10–1.15$, the threshold for cluster dissociation is exhibited on the time scale of ≈2–20 ps (fig. 4). In an extreme case, when extra excited-state repulsive interactions are switched off, i.e. when $\bar{\sigma} = 1.20$, the onset for dissociation is exhibited on the 1 ps time scale and is complete within 10 ps.

From these MD results the following picture concerning vibrational energy flow and reactive dynamics of the Ar_{13} cluster emerges. The temporal persistence of the vibrational excitation of the excimer (fig. 2) and of the "reaction centre" (fig. 3) corresponds to a "mode selective" excitation of the excimer, with vibrational energy redistribution within the cluster being precluded by two effects. First, the difference in the characteristic frequencies of the (high frequency) dimer motion and the (low frequency) motion of the cluster. Second, the local dilation of the cluster structure around the excimer, which is induced by the short-range excimer–cluster repulsive interactions. The vibrational energy flow from the dimer into the cluster (figs. 2 and 3) consists of two stages.

(A) Ultrafast vibrational energy transfer due to repulsion, which occurs on the time scale of ≈200 fs (figs. 2 and 3). This energy transfer process is dominated by the magnitude of the scale parameter $\bar{\sigma}$, being prominent for $\bar{\sigma} = 1.10–1.20$, with the amount of energy transferred from the excimer to the cluster decreasing with decreasing $\bar{\sigma}$ in the range $\bar{\sigma} = 1.20–1.10$, while the characteristic time scale for the process is practically invariant with respect to changes of $\bar{\sigma}$ in this narrow range. For $\bar{\sigma} = 1.00$ this process is switched off.

(B) "Slow" energy transfer on the time scale of tens of picoseconds (for $\bar{\sigma} = 1.20$) and up to hundreds of picoseconds (for $\bar{\sigma} = 1.00$) due to vibrational relaxation of the excimer.

The dynamics of the cluster induced by these energy transfer processes involves reactive vibrational predissociation, as is apparent from figs. 3 and 4. This state of affairs is, of course, drastically different from that encountered in infinite systems, where a nonreactive process prevails when the phonon modes of the system are excited. A cursory examination of the dissociative dynamics (fig.4) of the Ar_{13} cluster fol-

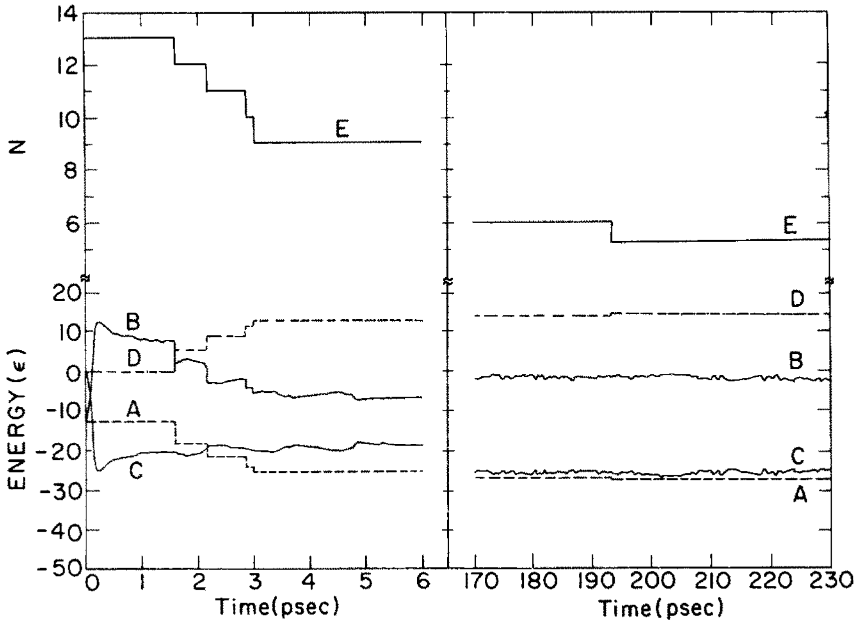

Fig. 3. Time evolution of fragmentation dynamics of the electronically excited $(Ar)_{13}$ cluster ($\bar{\sigma}$ = 1.15). (A) Total energy of the main fragment. (B) Total energy of the "bath subsystem". (C) Total energy of the "reaction centre". (D) Kinetic energy of the dissociated atoms. (E) Number of atoms in the main fragment. The steps in curves (A), (D) and (E) mark the stepwise dissociation of individual Ar atoms from the main fragment.

lowing excimer formation indicated that two reactive processes prevail.

(C) A fast stepwise "evaporation" of Ar atoms is exhibited on the time scale of ≈10 ps.

This process is induced by the energy transfer process (A). Subsequently, an additional reactive process appears (fig. 4), which involves:

(D) Slower vibrational predissociation of Ar atoms on the time scale ≥10 ps. This dissociative process is induced both by energy transfer processes (A) and (B).

It is imperative to note that the short-time "explosion" of the electronically excited cluster is induced by energy transfer due to short-range repulsive interactions. When these interactions are switched off by taking $\bar{\sigma}$ = 1.00, only mechanism (B) is operative for vibrational energy flow into the cluster and the cluster dissociative process, which again occurs by stepwise "evaporation" occurring on the time scale of 100–1000 ps. The appropriate excited-state repulsive physical parameter characterizing excimer–cluster interactions in RGCs is $\bar{\sigma}$ = 1.10–1.20, and we expect the occurrence of energy flow predissociation induced by excited repulsive interactions to occur on the time scale ≈10 ps. These predictions have not yet been subjected to an experimental test.

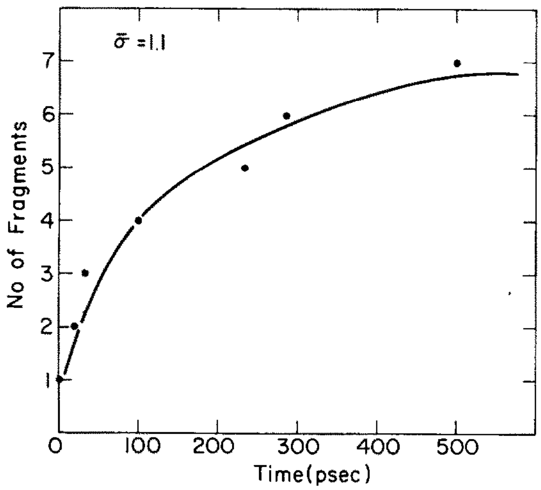

Fig. 4. The time evolution of the fragmentation of the electronically excited $(Ar)_{13}$ cluster ($\bar{\sigma}$ = 1.10). Note the sequential "evaporation" of the single grond-state Ar atoms.

We conclude this analysis of molecular dynamics in electronically excited states of RGCs with several comments. Firstly, a new mechanism of ultrafast vibrational energy flow induced by short-range repulsions has been documented. This mechanism will be of considerable importance for energy exchange between an extravalence (Rydberg) excitation and a cluster. Secondly, in small ($n = 13$) clusters the consequences of vibrational energy flow into the cluster involve a reactive dissociative process. Reactive vibrational predissociation manifests the dynamic consequence of vibrational energy flow into small clusters. Another extreme situation corresponds to infinite systems, where non-reactive vibrational energy redistribution prevails. It will be extremely interesting to increase the cluster size to establish the "transition" from reactive vibrational predissociation and "non-reactive" vibrational excitation of the cluster modes. Recent MD simulation on the dynamics of $Ar_{11}Xe_2^*$ and $Ar_{53}Xe_2^*$ clusters have established the "transition" from the reactive molecular-type behaviour in small clusters to the solid-state-type non-reactive behaviour in the large cluster [23]. Thirdly, the $Ar_{11}Ar_2^*$ electronically excited cluster provides an example of a system where "statistical" vibrational energy redistribution does not occur. The "mode selective" excitation of the excimer in the cluster constitutes a nice example for the violation of vibrational energy equipartitioning in a large finite system.

Acknowledgement

This research was supported in part by the United States Army through its European Research Office (to JJ), and by the US Department of Energy, Grant No. DE-FG05-86ER45234 (to UL).

References

[1] J. Jortner, Ber. Bunsenges. Physik. Chem. 88 (1984) 188.
[2] H. Haberland, Surface Sci. 156 (1985) 305.
[3] J.J. Sâenz, J.M. Soler and N. Garcia, Surface Sci. 156 (1985) 121.
[4] J.J. Sâenz, J.M. Soler, N. Garcia and O. Echt, Chem. Phys. Letters 109 (1984) 71.
[5] E.E. Polymeropoulos and J. Brickmann, Surface Sci. 156 (1985) 563.
[6] U. Landman, D. Scharf and J. Jortner, Phys. Rev. Letters 54 (1985) 1860.
[7] J.W. Brady and J.D. Doll, J. Chem. Phys. 73 (1980) 2767.
[8] S.A. Rice, Advan. Chem. Phys. 47 (1982) 117.
[9] M.F. Vernon, D.J. Kraynovich, H.S. Kwok, J.M. Lisy, Y.R. Shen and Y.T. Lee, J. Chem. Phys. 77 (1982) 47.
[10] N. Schwentner, E.E. Koch and J. Jortner, Electronic excitations in condensed rare gases. Springer tracts in modern physics, Vol. 107 (Springer, Berlin, 1985).
[11] J. Jortner, E.E. Koch and N. Schwentner, in: Photophysics and photochemistry in the Vacuum Ultraviolets, eds. S.P. McGlynn, G.L. Findley and R.H. Huebner (Reidel, Dordrecht, 1985) p. 515.
[12] J.R. Beeler and G.L. Kulcinski, in: Interatomic potentials and simulation of lattice defects, eds. P.C. Gehlen, J.R. Beeler and J. Jaffee (Plenum Press, New York, 1972) p. 735.
[13] A. Raman and F.H. Stillinger, J. Chem. Phys. 55 (1971) 3336.
[14] F.G. Amar and B.J. Berne, J. Phys. Chem. 88 (1984) 6720.
[15] W.D. Kristensen, E.J. Jensen and M.J. Cotterill, J. Chem. Phys. 60 (1974) 4161.
[16] K.T. Gillen, R.P. Saxon, D.C. Lorentz, G.E. Ice and R.E. Olson, J. Chem. Phys. 64 (1976) 1925.
[17] I. Messing, B. Raz and J. Jortner, J. Chem. Phys. 66 (1977) 2239, 4577.
[18] G.L. Briant and J.J. Burton, J. Chem. Phys. 63 (1975) 2045.
[19] N. Quirke and P. Sheng, Chem. Phys. Letters 110 (1984) 63.
[20] J.B. Kaelberer and R.D. Etters, J. Chem. Phys. 66 (1977) 3233.
[21] M.R. Hoare and P. Pal, Advan. Chem. Phys. 40 (1979) 49.
[22] A. Nordsieck, Math. Comp. 16 (1962) 22.
[23] D. Scharf, J. Jortner and U. Landman, to be published.